Observation of inter-Landau-level transitions in resonant tunneling between transverse *X* states in GaAs/AlAs double-barrier structures under hydrostatic pressure

J. M. Smith* and P. C. Klipstein
Clarendon Laboratory, Department of Physics, University of Oxford, Parks Road, Oxford OX1 3PU, United Kingdom

R. Grey and G. Hill
Department of Electrical and Electronic Engineering, University of Sheffield, Mappin Street, Sheffield S1 3JD, United Kingdom
(Received 10 April 1997)

We have carried out sensitive measurement of the vertical transport characteristics of several GaAs/AlAs ''double-barrier'' heterostructures pressurized just beyond the type-II transition, and in the presence of longitudinal magnetic fields of up to 15 T. Towards the upper field limit, clear periodic structure is observed in the second derivative current-voltage characteristic of the resonance attributed to the process $X_t(1) \rightarrow X_t(1) + \mathrm{TO}_{\mathrm{AlAs}}$, where $X_t(1)$ indicates the lowest quasiconfined subband associated with the transverse *X* minima in AlAs, and $\mathrm{TO}_{\mathrm{AlAs}}$ is a zone center transverse optical phonon. The periodic structure is interpreted as a series of transitions to collector states of increasing Landau index, with the requirement for conservation of in-plane momentum being satisfied for any interlevel transition by the phonon emission. Quantitative analysis of the data yields a value for the Landau-level separation, and thus also a value for the two-dimensional geometric effective mass of the transverse *X* minima in AlAs. [S0163-1829(98)01803-7]

I. INTRODUCTION

The application of longitudinal magnetic fields to simple heterostructures in order to view inter-Landau-level tunneling processes in the $Al_xGa_{1-x}As$ system has until recently been limited to the Γ point of the Brillouin zone (BZ).[1,2] However, the *X* point minima in AlAs are known to be significant in limiting the quality of the current resonances displayed by GaAs/AlAs double-barrier resonant tunneling diodes (DBRTD's),[3–6] and so there is considerable interest in their similar characterization.

A study was carried out last year by Finley *et al.*[7] in which they observed tunneling through Landau levels of the longitudinal $X_l(1)$ subband in a GaAs/AlAs single-barrier structure. This paper now reports measurement of tunneling between Landau levels of transverse subbands. To do this, it was necessary to employ hydrostatic pressure for the controled population of the quasibound *X* states by effecting a type-I to type-II transition, and high-resolution phase-sensitive techniques to resolve the small Landau-level separations associated with the large effective masses of the *X* minima.

A detailed study of the full range of tunneling processes displayed by the device reported here is presented in another paper.[8] The paper also describes how quantitative calibration of the resonance bias positions to the relative potential between the two *X* wells is carried out using a self-consistent Schrödinger-Poisson model.

II. EXPERIMENT

The four samples involved in the study[8] were nominally symmetric *n-i-n* GaAs/AlAs DBRTD's grown by molecular-beam epitaxy on [100] oriented substrates. They were nominally identical with the exception of the AlAs layer thicknesses, which were varied in 10 Å increments between 40 and 70 Å.

Of the four samples, the one with the 70 Å AlAs layers has $X_t(1)$ both as ground states in each well of the conduction-band profile and separated by the largest energy from the higher $X_t(1)$ state, and therefore displays the most purely transverse characteristics. It is perhaps for this reason that it was the only one to show clearly the inter Landau-level processes. The constituent epitaxial layers of this sample were as follows: 0.25 μm, $n=1\times10^{18}$ cm^{-3} GaAs:Si buffer, 0.5 μm, $n=2\times10^{17}$ cm^{-3} GaAs:Si, 100 Å undoped (ud) GaAs spacer, 70 Å ud AlAs, 40 Å ud GaAs, 70 Å ud AlAs, 100 Å ud GaAs spacer, 0.5 μm $n=2\times10^{17}$ cm^{-3} GaAs:Si, 0.25 μm $n=1\times10^{18}$ cm^{-3} GaAs:Si cap. Mesa diameters were 20 μm.

All measurements presented here were taken at a pressure of 10.2 kbar, which is some 1.5 kbar past the type-I to type-II transition pressure of the sample, and at a temperature of 4.2 K. Hydrostatic pressure was applied using a clamp cell, equipped with an *in situ* manganin wire manometer. The two terminal transport measurements were carried out using a combined voltage source and virtual ground current amplifier system. Conductance and second derivative current-voltage measurements were made by modulating the applied voltage with a sinusoid of 1 mV rms, and $\sim$1 kHz, and subsequently detecting the same frequency or double frequency ac signal with a lock-in amplifier.

Orientation of the crystal relative to the magnetic field was carried out manually and by eye under a microscope, due to the constraints imposed by the pressure cell. The estimated deviation from coaxial alignment is therefore $\pm5°$. Additionally to the results published here, magnetotunneling measurements were performed with in-plane magnetic-field orientation, and these are to be presented separately.[9]

III. RESULTS AND ANALYSIS

The current-voltage (I-V) and conductance-voltage (I'-V) characteristics of the sample under these conditions,

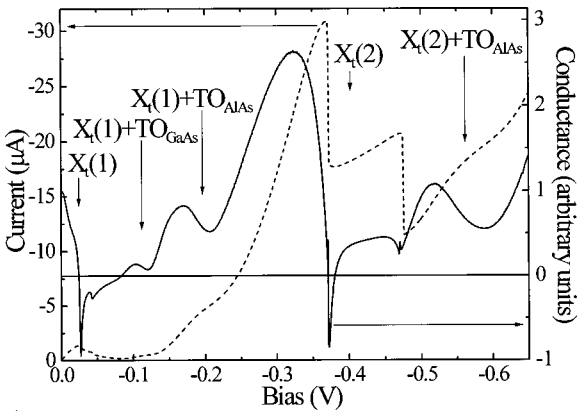

FIG. 1. Reverse bias I-V (broken line) and I'-V (solid line) characteristics of the sample in the absence of a magnetic field, and at a pressure of 10.2 kbar and a temperature of 4.2 K. The collector states responsible for each of the observed resonant features are given. Note that the double step in the I-V characteristic of the $X_t(2)$ resonance is merely the well-known product of the measuring circuit in a region of strong negative differential resistance.

and with $B=0$, are shown in Fig. 1. Five resonant processes have been identified, each with an $X_t(1)$ emitter state, and having collector states, in order of increasing absolute bias, of $X_t(1)$, $X_t(1)+\mathrm{TO_{GaAs}}$, $X_t(1)+\mathrm{TO_{AlAs}}$, $X_t(2)$, and $X_t(2)+\mathrm{TO_{AlAs}}$.[8] It is perhaps important to state here that the degree of accuracy in the model appears to be sufficient to distinguish between the zone-center phonon energies of the TO and LO branches in both materials.

Figure 2 shows the combined potential profiles of the Γ and X point conduction-band minima, with the sample at the temperature and pressure stated above, and biased so that the resonant process $X_t(1)\rightarrow X_t(1)+\mathrm{TO_{AlAs}}$ is energetically aligned. The continuity of the Fermi energy between the contact and the emitter AlAs layer is a consequence of the relative transparency of the δ barrier compared with the central X-like barrier. Note that it is more probable that phonon emission for the tunneling process will occur in the collector layer as opposed to the emitter layer, since in the latter case the tunneling barrier height is larger by an amount equal to

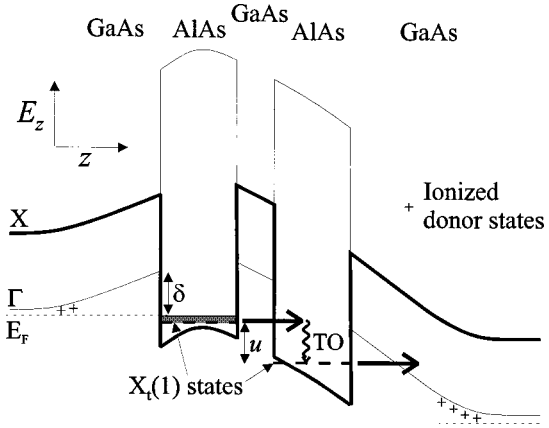

FIG. 2. Band profile diagram for the GaAs/AlAs DBRTD pressurized beyond the type-II transition and biased to the $X_t(1)\rightarrow X_t(1)+\mathrm{TO_{AlAs}}$ resonance, the pressure. The presence of the δ barrier as a result of Fermi level pinning in the emitter, and the definition of the u value, are included. (Not to scale.)

the phonon energy, resulting in greater attenuation of the wave function. We define the parameter u as the energy difference between the two $X_t(1)$ states.

Upon application of a longitudinal magnetic field [B parallel to the growth (z) direction] the in-plane energy $E_{x,y}$, of the electron states is quantized into Landau levels so that

$$E_{x,y}=\left(n+\frac{1}{2}\right)\frac{\hbar eB}{m^*_{\mathrm{geo}}}. \tag{1}$$

Here m^*_{geo} is the two-dimensional (2D) geometric average effective mass in the plane of the layers, which, in the case of the four transverse X minima, if they are truly elliptical, is equal to $(m^*_{X,L}m^*_{X,T})^{1/2}$, where $m^*_{X,L}$ and $m^*_{X,T}$ are the respective principal effective masses parallel with, and perpendicular to, the long wave vector of a given X minimum. Current estimates for their values are $(1.1\pm0.2)m_0$ and $(0.24\pm0.05)m_0$, respectively.[7,8,10] n is the Landau index ($n=0,1,2,\ldots$.).

The electron density contained in the fourfold degenerate emitter $X_t(1)$ state when this resonant process is aligned, as in Fig. 2, is calculated by Poisson's equation to be around 4×10^{15} m^{-2}. At a magnetic field of 8 T, below which no inter-Landau-level transitions are resolved, the number of states per Landau level is $4\times2eB/h=1.6\times10^{16}$ m^{-2}, and the level separation is expected to be around 1.5 meV. Thus for all of the inter-Landau-level measurements made here (at 4.2 K, $k_BT=0.3$ meV), only the $n=0$ emitter Landau level is occupied. Optical phonon emission can couple this emitter wave function with an $X_t(1)$ collector state of any Landau index, as the phonon dispersion includes states at all values of in-plane momentum. Moreover, the phonon dispersion near to the zone center is small enough that the energy of the phonons involved in different inter-Landau-level processes can be taken as constant. The u value for each process therefore depends on the amount of energy required for the in-plane motion of the collector state, and is given by the expression

$$u=E_{\mathrm{TO}}+n\frac{\hbar eB}{m^*_{\mathrm{geo}}}, \tag{2}$$

where E_{TO} is the $\mathrm{TO_{AlAs}}$ zone-center phonon energy, and $n=0,1,2,\ldots$.

The second derivative current-voltage (I''-V) characteristics in the vicinity of the $X_t(1)\rightarrow X_t(1)+\mathrm{TO_{AlAs}}$ reverse bias (substrate acting as emitter) resonance, for magnetic fields of zero and 15 T, are displayed in Fig. 3(a). It is the minima of these curves that are expected to correspond with resonant alignment, and at zero field this can clearly be seen to occur at an applied bias of around -185 mV. At 15 T, this minimum has barely changed, while three further minima have developed at regular intervals of bias above the parent minimum. To observe the development of these features with magnetic field, it is helpful to subtract the slowly varying background from the high-field curves. In Fig. 3(b), the curve measured at 8 T has been used for this purpose, since it occurs just prior to the resolution of the new features.

By using the Schrödinger-Poisson model,[8] the bias scale of these curves has been calibrated against u. The calibration is based on a phonon energy of 42 meV. The u values of the

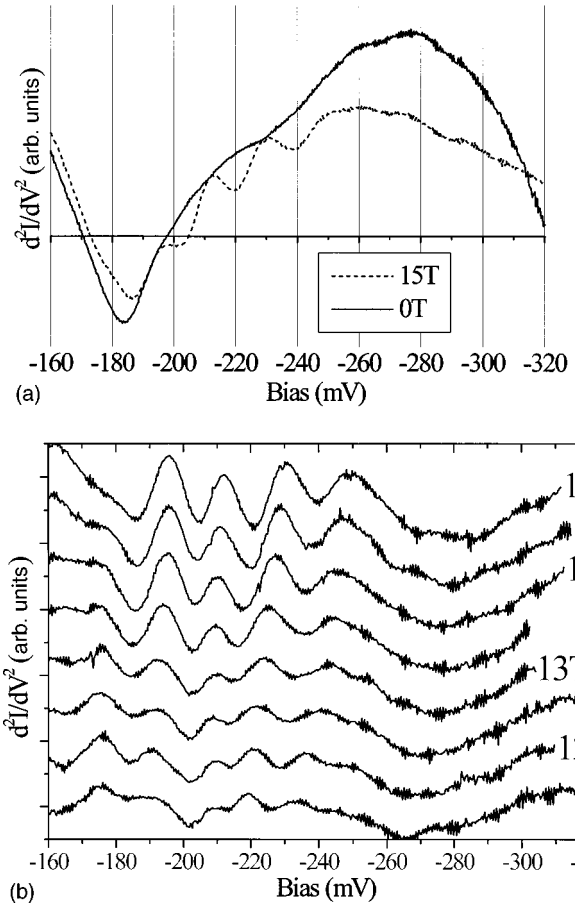

FIG. 3. (a) Second derivative current-voltage measurements at magnetic fields of zero and 15 T applied parallel to the z direction, for 10.2 kbar pressure at 4.2 K. Alignment of the $X_t(1) \rightarrow X_t(1) + \mathrm{TO}_{\mathrm{AlAs}}$ resonance is indicated by the minimum at around -185 mV, and three further minima are clearly visible at high field. (b) Second derivative current-voltage curves for the sample in Fig. 3(a) at magnetic fields between 11.5 and 15 T, after subtraction of the 8 T curve. This provides a better view of the development of the inter-Landau-level processes than does the raw data of Fig. 3(a).

minima of the curves in Fig. 3(b) are plotted against magnetic field in Fig. 4, revealing the fan of resonances described by Eq. (2). Varying m^*_{geo} in Eq. (2), to obtain the closest fit to these data points (solid lines), yields a value of $m^*_{\mathrm{geo}} = 0.56 m_0$. We estimate that the error in the phonon energy is ± 2 meV,[8] which can be shown to correspond to an error in the effective mass of $\pm 7\%$, or that $m^*_{\mathrm{geo}} = (0.56 \pm 0.04) m_0$. This is in good agreement with the values stated earlier for the two principal masses of the X minima in AlAs.

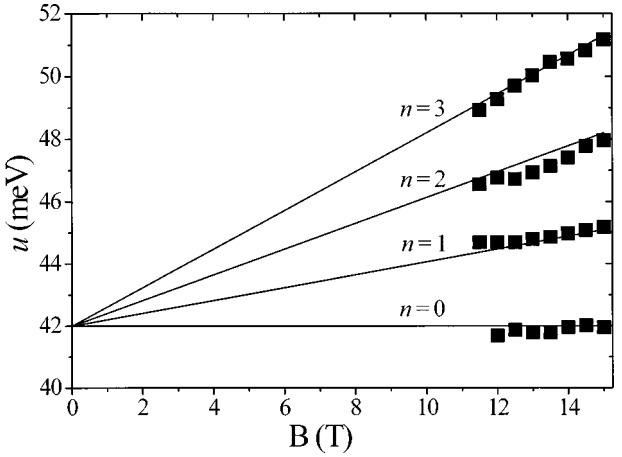

FIG. 4. Comparison between the measured u-values (squares) and the field dependence of u that is predicted from Eq. (2) using the best-fit mass of $m_{\mathrm{geo}} = 0.56 m_0$ (solid lines).

IV. SUMMARY

Sensitive vertical transport measurements have revealed tunneling resonances resulting from the inter-Landau-level transitions between transverse X states in a type-II GaAs/AlAs DBRTD. The resonant process that allows these transitions has been separately attributed to $X_t(1) \rightarrow X_t(1) + \mathrm{TO}_{\mathrm{AlAs}}$, and the interlevel transitions themselves involve an emitter state of Landau index $n = 0$, and collector states of indices $n = 0$, 1, 2, and 3. Calibration of the bias scale to find the Landau-level separation has yielded a value of the 2D geometric average effective mass for the transverse X minima of $m^*_{\mathrm{geo}} = (0.56 \pm 0.04) m_0$, in good agreement with that expected in the light of previous measurements.

ACKNOWLEDGMENTS

This work was funded by the Engineering and Physical Sciences Research Council (EPSRC), and J.M.S. acknowledges additional support from the General Electric Company (GEC). We also thank Professor M. E. Eremets for his work in the design and construction of the pressure cell.

*Present address: Research Dept. (0500), Electronics and Telecommunications Research Institute (ETRI), 161 Kajong-dong-Gu, Taejon 305-350, S. Korea.

[1] J. Smoliner, E. Gornik, and G. Weimann, Phys. Rev. B **39**, 12 937 (1989).
[2] C. H. Yang, M. J. Yang, and Y. C. Kao, Phys. Rev. B **40**, 6272 (1989).
[3] I. Hase, H. Kawai, K. Kaneko, and N. Watanabe, J. Appl. Phys. **59**, 3792 (1986).
[4] E. E. Mendez, E. Calleja, C. E. T. Gonçalves da Silva, L. L. Chang, and W. I. Wang, Phys. Rev. B **33**, 7368 (1986).
[5] P. M. Solomon, S. L. Wright, and C. Lanza, Superlattices Microstruct. **2**, 521 (1986).
[6] A. R. Bonnefoi, T. C. McGill, R. D. Burnham, and G. B. Anderson, Appl. Phys. Lett. **50**, 344 (1987).
[7] J. J. Finley, R. J. Teissier, M. S. Skolnick, J. W. Cockburn, R. Grey, G. Hill, and M. A. Pate, Phys. Rev. B **54**, R5251 (1996).
[8] J. M. Smith, P. C. Klipstein, R. Grey, and G. Hill, preceding paper, Phys. Rev. B **57**, 1740 (1998).
[9] J. M. Smith, P. C. Klipstein, R. Grey, and G. Hill (unpublished).
[10] S. Adachi, *GaAs and Related Materials; Bulk Semiconducting and Superlattice Properties* (World Scientific, Singapore, 1994).